

# New pathway ameliorating ulcerative colitis: focus on *Roseburia intestinalis* and the gut–brain axis

Fenghua Xu, Yi Cheng, Guangcong Ruan, Liqin Fan, Yuting Tian, Zhifeng Xiao, Dongfeng Chen and Yanling Wei 

Ther Adv Gastroenterol

2021, Vol. 14: 1–14

DOI: 10.1177/  
17562848211004469

© The Author(s), 2021.  
Article reuse guidelines:  
sagepub.com/journals-  
permissions

## Abstract

**Background:** The community of gut microbes is a key factor controlling the intestinal barrier that communicates with the nervous system through the gut–brain axis. Based on our clinical data showing that populations of *Roseburia intestinalis* are dramatically decreased in the gut of patients with ulcerative colitis, we studied the efficacy of a strain belonging to this species in the context of colitis and stress using animal models.

**Methods:** Dextran sulfate sodium was used to induce colitis in rats, which then underwent an enema with *R. intestinalis* as a treatment. The disease activity index, fecal changes and body weight of rats were recorded to evaluate colitis, while histological and immunohistochemical analyses were carried out to examine colon function, and 16S rRNA sequencing was performed to evaluate the gut microbiota change. Behavioral assays and immunohistochemical staining of brain were performed to assess the effect of *R. intestinalis* on the gut–brain axis.

**Results:** Colitis-related symptoms in rats were significantly relieved after *R. intestinalis* enema, and the stool traits and colon length of rats were significantly recovered after treatment. The gut epithelial integrity and intestinal barrier were restored in treated rats, as evidenced by the higher expression of Zo-1 in colon tissues, accompanied by the restoration of gut microbiota. Meanwhile, depressive-like behaviors of rats were reduced after treatment, and laboratory experiments on neuronal cells also showed that IL-6, IL-7 and 5-HT were downregulated by *R. intestinalis* treatment in both serum and brain tissue, while Iba-1 expression was reduced in treated rats.

**Conclusions:** The administration of *R. intestinalis* contributes to restoration of the gut microbiota, promoting colon repair and the recovery of gastrointestinal function. These alterations are accompanied by the relief of depressive-like behaviors through a process modulated by the neuronal network and the regulation of inflammation by the gut–brain axis.

**Keywords:** gut–brain axis, gut microbiota, probiotic, *Roseburia intestinalis*, ulcerative colitis

Received: 17 February 2021; revised manuscript accepted: 4 March 2021.

## Introduction

Ulcerative colitis (UC) is a chronic and relapsing disease of the intestinal tract that substantially decreases patients' quality of life.<sup>1</sup> In addition to diarrhea, abdominal pain, malnutrition and other gastroenterological abnormalities, psychiatric disorders are also associated with UC.<sup>2</sup> Dysbiosis of

the gut microbiota was shown to induce mental health disorders through the gut–brain axis by modulating the inflammatory response, neuronal network or immunological regulation.<sup>3</sup> Clinical studies have indicated that the incidence of fatigue, anxiety, depression, and other psychiatric disorders is significantly higher in patients with

Correspondence to:

**Yanling Wei**  
Department of  
Gastroenterology, Army  
Medical Center of PLA  
Affiliated with Army  
Medical University,  
Chongqing 400042, China  
[lingzi016@126.com](mailto:lingzi016@126.com)

**Fenghua Xu**  
**Yi Cheng**  
**Guangcong Ruan**  
**Liqin Fan**  
**Yuting Tian**  
**Zhifeng Xiao**  
**Dongfeng Chen**  
Department of  
Gastroenterology, Army  
Medical Center of PLA  
Affiliated with Army  
Medical University,  
Chongqing, China

UC than in healthy controls.<sup>4–6</sup> Although the cause and effect of neurological disorders associated with UC are unclear, clinical trials have suggested that the remission of digestive diseases is often accompanied by the relief of mental health disorders.<sup>7,8</sup>

To date, the pathogenesis and etiology of UC are not clear and might involve genetic, environmental and immunological factors.<sup>9–11</sup> As the intestinal mucosa is a complicated environment where the gut microbiome plays a vital role in intestinal functioning, dysbiosis of the gut microenvironment is closely related to the incidence of UC.<sup>12,13</sup> The depletion of “anti-inflammatory” taxa has been observed in patients with UC, along with expansion of proinflammatory microorganisms.<sup>14</sup>

Microbiota modulation for the treatment of colitis is a hot research topic,<sup>15,16</sup> and various reports have proven that probiotic bacteria exert a satisfactory effect on repairing the intestinal barrier and can help reestablish intestinal homeostasis.<sup>17</sup> Recently, our clinical data revealed that the abundance of *Roseburia intestinalis* is significantly decreased in patients suffering from colitis. *R. intestinalis* is a butyrate-producing obligate anaerobe that belongs to the *Roseburia* genus in *Clostridium* cluster XIVa of the Firmicutes phylum, which is essential for host metabolism.<sup>18,19</sup> Recent studies of animal models of colitis have also suggested that *R. intestinalis* exerts a positive effect on colitis by suppressing inflammatory immune responses and improving the gut barrier.<sup>20,21</sup>

However, researchers have not determined whether *R. intestinalis* might act on colitis and the nervous system to ameliorate dysbiosis-related neurological disorders through the gut–brain axis. Here, we hypothesize that the restoration of gut microbiota by *R. intestinalis* might protect the nervous system. Our work aims to assess whether *R. intestinalis* protects rats from mental health conditions caused by gut dysfunction.

## Materials and methods

### *Fecal biodiversity analysis on an ulcerative patient*

One male patient aged 52 years was diagnosed with UC and underwent fecal microbiota transplantation (FMT) using FMT capsules (patent NO. ZL201510304041.4). Colonoscopy was

carried out to evaluate UC before and after FMT treatment. Stool samples were collected from this patient before and after FMT treatment and stored at  $-80^{\circ}\text{C}$  until a further gut microbiota analysis using 16S rRNA sequencing. Stool samples were sent to G-Bio, Hangzhou, China for 16S rRNA sequencing and an analysis of the stool composition.

### *Roseburia intestinalis culture and identification*

*R. intestinalis* (DSMZ-14610) (Deutsche Sammlung von Mikroorganismen und Zellkulturen GmbH, Braunschweig, Germany) was used in this study and stored in cryotubes at  $-80^{\circ}\text{C}$ . The bacteria were grown under strict anaerobic conditions at  $37^{\circ}\text{C}$  for 24 h in BD BACTEC Lytic/10 Anaerobic/F medium (Becton Dickinson and Company, United States) until they reached the stationary phase and a working culture was obtained.

*R. intestinalis* samples were sent to BGI genomics (Shenzhen, China) for 16S rRNA sequencing using 16S primers: 27f (AGAGTTTGATCMTGGCTCAG) and 1492R (TACGGYTACCTGTTACGACTT). The sequencing results were compared with the NCBI sequence database to identify the strain using the Basic Local Alignment Search Tool (BLAST).

### *Morphology of R. intestinalis*

The morphology of the *R. intestinalis* cells was analyzed using Gram staining and scanning electron microscopy (SEM).

The sample was prepared for the SEM analysis as described below. The isolated and purified bacteria were inoculated in a shake flask containing 40 ml of BD BACTEC™ Lytic/10 Anaerobic/F Culture Vials liquid medium and cultured without shaking for 48 h. After culture, 500  $\mu\text{l}$  of the bacterial solution were aspirated and centrifuged at 3000 rpm for 3 min. The supernatant was removed, and 800  $\mu\text{l}$  of phosphate-buffered saline (PBS) were added to wash the pellet 2–3 times. Then, 1 ml of 2.5% glutaraldehyde was added to the precipitate, and the sample was mixed and incubated at  $4^{\circ}\text{C}$  overnight; the sample was centrifuged at 3000 rpm for 3 min, and the supernatant was removed. Gradient ethanol dehydration was performed with a 20%, 50%, 80%, and 100%

ethanol, with dehydration for 10 min each, and centrifugation was performed at 3000 rpm for 3 min; then, 100% 2-methyl-2-propanol was added 2–3 times for washing, and the samples were observed using SEM.

For Gram staining, the bacterial suspension was fixed on glass slides using a flame. Crystal violet solution A was added and incubated for 2 min. The slide was washed with running water to remove the excess dye. Iodine-potassium iodide solution B was added and incubated for 5 min. The slide was washed with running water. Excess water was allowed to run off, and then the sections were immediately placed in absolute acetone. Four changes of absolute acetone were used for a total of 100 s. The sample was briefly washed with running water until the acetone was removed. Carbol-fuchsin solution C was added and incubated for 1–11 min, followed by a brief wash with running water, and the sample was observed after drying.

#### *Animals and groups*

Adult male Sprague-Dawley rats were purchased from the Experimental Animal Center, Institute of Field Surgery, Committee of Army Medical Center, and housed at 22°C on a 12:12-h light-dark cycle with free access to water and food. The rats were randomly assigned to the following groups ( $n=10$  per group): control, dextran sodium sulfate (DSS) alone, and DSS plus *R. intestinalis* (DSS + R.I). The control rats were fed sterile drinking water daily. The rats in the DSS group were treated with 4% DSS daily for 7 days, followed by sterile drinking water treatment (without DSS) for 7 days. The rats in the DSS + R.I group were treated with 4% DSS daily for 7 days and then treated with *R. intestinalis* daily for the next 7 days by enema. All experimental protocols were conducted in accordance with the recommendations of the Daping Hospital Animal Experiment Center Guidelines and Animal Ethics Committee of Daping Hospital affiliated with Army Medical University. The protocol (AMUWEC2020639) was approved by the Laboratory Animal Welfare and Ethics Committee of Third Military Medical University.

#### *Induction of colitis and R. intestinalis treatment*

The animals were allowed to adapt to the environment for 1 week before the experiment. The

whole experiment lasted for 17 days (Figure 3a). Specifically, 4% (w/v) DSS (M.W.: 36,000–50,000 Da, MP Biomedical, United States) in drinking water was used to induce acute colitis in rats for 7 days (DSS group), and the control group of rats received only regular sterile drinking water (control group). A freshly prepared DSS solution was administered every 2 days. Rats in the DSS + R.I group received  $10^9$  CFU/100  $\mu$ l of *R. intestinalis* enterally by enema for 7 days after challenge with DSS. The food and water/DSS consumption, weight, feces and living conditions were monitored daily. The disease activity index (DAI) was calculated by scoring changes in weight loss, stool consistency, and intestinal bleeding, according to the classic scoring system reported by Cooper *et al.*<sup>22</sup> On the 15th day, the rats were weighed and euthanized under anesthesia. Peripheral blood was collected and centrifuged ( $1500 \times g$ , 15 min), and the supernatant was frozen at  $-80^\circ\text{C}$  until further analysis using enzyme-linked immunosorbent assays (ELISAs). The colon was removed and measured. After rinsing with PBS, the colon was cut into several sections: some sections were fixed with 4% (w/v) paraformaldehyde for histopathological and immunohistochemical (IHC) staining, and the others were fixed at  $-80^\circ\text{C}$  and frozen for western blotting analysis, ELISA and quantitative reverse transcription PCR (qRT-PCR).

#### *Behavioral tests*

Behavioral tests were performed 24 h after the last treatment as described in a previous report.<sup>23</sup> After 1 week of DSS exposure with or without 7 days of *R. intestinalis* treatment, the assays were conducted on three consecutive days in the following order: open field test (OFT), tail suspension test (TST) and light/dark box (LDB) test.

*Open field test.* Each rat was gently placed in a  $100 \times 100 \times 45$  cm square box. The bottom of the box was divided into 25 small squares, and the nine small center squares were defined as the central area and the other 16 squares as the peripheral area. Each rat was slowly placed into the box along the corner of the wall and allowed to explore the apparatus for 15 min. During the experiment, the chamber was kept quiet, and the box was cleaned after testing. Movements were digitally captured and analyzed using EthoVision XT video tracking software (Noldus Information Technology, Inc., Netherlands) to evaluate the

rat's ability to explore the center or surrounding area and the walking distance.<sup>23</sup>

*Tail suspension test.* The TST involves a transparent square box with hooks. Approximately 1 cm of the rat's tail was taped on the hook, and the rat was hung upside down 40 cm from the ground. The suspension lasted for 6 min; the first minute was considered the adaptive time (latency period), and the recording continued from the 2nd to the last minute. During the experiment, the room was kept quiet. Movements were digitally captured and analyzed using EthoVision XT video tracking software to assess the rats in a state of immobility.<sup>23</sup>

*Light/dark box.* The LDB assay was performed as previously reported.<sup>24</sup> Rats were individually placed in a light and dark box apparatus, that is, a box (60 × 30 × 30 cm) divided into a dark area and a light area (30 × 30 cm each), and allowed to explore for 10 min. Rats were placed in the light area and allowed to move freely. The time spent in the dark side and the number of transitions between the light side and dark side were evaluated.

#### *Hematoxylin-eosin staining (H&E)*

Harris' hematoxylin (YuanYe Biotechnology, Shanghai, China) was used to stain the samples for 5 min, which were then gently washed with water. Differentiation was carried out for 5 s with a 1% hydrochloric acid alcohol solution (1 ml), and the color of the slice was observed to change from blue to red. Then, after the sections were washed with tap water for 1.5 h, they were stained with 0.5% eosin (water-soluble, Aladdin Bio-Chem Technology, Shanghai, China) for 2 min. After the aforementioned staining process, the sections were dehydrated with different concentrations of ethanol and cleared with 100% xylene. Cover slips were mounted over the sections before they were assessed under a microscope (Carl Zeiss, Oberkochen, Germany).

#### *Masson's trichrome staining*

After 5 min of staining with Harris' hematoxylin, the sections were washed with running water. The samples were differentiated with 1% hydrochloric acid for 1 min and then rinsed for 1.5 h. Next, Ponceau (Aladdin Bio-Chem Technology, Shanghai, China) was added for 7 min, and

distilled water was used for washing. The samples were treated with a 1% aqueous solution of phosphomolybdic acid (Fuguang Fine Chemical Research Institute, Tianjin, China) for approximately 5 min without washing with water and directly counterstained with an aniline blue (Aladdin Bio-Chem Technology, Shanghai, China) solution for 5 min. Finally, the sample was treated with 1% glacial acetic acid (Tianjin Tianli Chemical Reagent Co., Tianjin, China) for 1 min and shaken. After staining, the slices were dehydrated with different concentrations of ethanol and cleared with 100% xylene. Cover slips were mounted over the sections before they were assessed under a microscope.

#### *Immunohistochemical staining*

The histological sections were subjected to antigen retrieval, cooled for 2 h, treated with 0.3% (w/v) H<sub>2</sub>O<sub>2</sub> for 15 min, blocked with PBS containing 5% (w/v) bovine serum and 0.1% (w/v) Triton X-100 for 15 min, and incubated with a goat anti-Iba-1 antibody (1:500, Abcam, United Kingdom), rabbit anti-Zo1 antibody (1:500, Abcam, United Kingdom) or mouse anti-GFAP antibody (1:500, Sigma-Aldrich, United States) overnight at 4°C. After the sections were washed, they were incubated with biotinylated secondary antibodies (1:200, Thermo Fisher Scientific, United States) for 1 h, followed by staining with the avidin-biotin-peroxidase complex (ABC, Vector Laboratories, United States). The diaminobenzidine (DAB) reaction was visualized from the immunoprecipitated product. After the aforementioned staining procedures, the sections were dehydrated with different concentrations of ethanol and cleared with 100% xylene. Cover slips were mounted over the sections, which were then assessed under a microscope (Carl Zeiss, Oberkochen, Germany).

#### *Western blotting*

Proteins were extracted from the brains and intestinal tissues using RIPA lysis buffer (KeyGen Biotech, Nanjing, China) containing phenylmethylsulfonyl fluoride (Biosharp Life Sciences, Hefei, China) and a phosphatase inhibitor cocktail (MedChemExpress, Shanghai, China). The total protein concentration was determined with a BCA Protein Assay Kit (KeyGen Biotech, Nanjing, China). For western blotting, the samples (30 mg protein) were separated on 10% (w/v) acrylamide SDS-PAGE gels

and then transferred to a nitrocellulose membrane (Pall Corporation, United States). The membrane was then blocked with 5% (w/v) BSA (Gentihold, Beijing, China) before an overnight incubation with goat anti-Iba-1 (1:500, Abcam), mouse anti-GFAP (1:500, Sigma-Aldrich), rabbit anti-ZO1 (1:500, Abcam), and mouse anti- $\beta$ -actin (1:500, Santa Cruz Biotechnology, United States) primary antibodies at 4°C. After three washes for 10 min with Tris-buffered saline containing 0.1% (v/v) Tween 20 (TBST), the nitrocellulose membranes were incubated with a fluorescent dye-labeled secondary antibody (1:15000; LI-COR Biosciences, United States) for 60 min at room temperature. After the incubation with the appropriate secondary antibodies, the membranes were analyzed and quantified using an Odyssey CLx Imager and Image Studio software (LI-COR Biosciences).

#### *RNA extraction and qRT-PCR*

Total RNA was extracted from the brains and intestinal tissues using TRIzol reagent (Thermo Fisher Scientific, United States) according to the manufacturer's protocol. The RNA concentration was quantified using ultraviolet spectrophotometry at 260/280 nm (Nanodrop 2000, Thermo Fisher Scientific, United States). The PrimeScript First-Strand cDNA Synthesis Kit (Takara Bio, Japan) was used to reverse transcribe cDNAs. PCR was performed in an Mx3000P qPCR System (Agilent Technologies, United States) with the corresponding primers (Takara Bio, Japan) and SYBR Green PCR master mix (Takara Bio, Japan). The primer sequences were as follows: il-17a (sense primer: 5' TCAACCGTTCCA CTTCACCC 3', anti-sense primer: 5' ACTTC TCAGGCTCCCTCTTCAG 3'), il-6 (sense primer: 5' CAACGATGATGCACTTGCGAGA 3', anti-sense primer: 5' CTCCAGGTAGCTA TGGTACTCCAGA 3').

#### *Enzyme-linked immunosorbent assay*

The changes in the levels of cytokines and neurotransmitters in the serum, colon and intestine were determined using ELISAs. Blood samples were collected, stored at 4°C overnight and centrifuged at 3000 *g* for 20 min, and serum samples (supernatant) were collected for further experiments. ELISAs were performed according to the protocols provided with the IL-6, IL-17 and

5-HT kits (PeproTech, Rehovot, United States). An iMark Microplate Absorbance Reader (Bio-Rad, United States) was used to measure the absorbance at 450 nm.

#### *Analysis of the gut microbiota using 16S rRNA sequencing*

Rat stool samples were collected daily by stimulating the anus and were stored at -80°C. The stool samples and FMT bacterial fluid were sent together to Sangon Biotech (Shanghai, China) for 16S rRNA sequencing with the Illumina MiSeq platform. The biodiversity of the microbiota was analyzed by performing principal component analysis and clustering analysis.

#### *Statistical analysis*

SPSS statistics software 17.0 (SPSS, United States) was used for all quantitative analyses. Data are presented as the means  $\pm$  SE of the number (*n*) of samples analyzed in all experiments. Data with one variable were analyzed using one-way ANOVA with the Newman-Keuls *post hoc* test. Data with two variables were analyzed using two-way ANOVA with Tukey's *post hoc* test when appropriate. When significantly unequal variance existed, the data were transformed prior to statistical analysis. Statistical significance was established with  $\alpha=0.05$ , \*indicates " $p < 0.05$ ", \*\*indicates " $p < 0.01$ " and \*\*\*indicates " $p < 0.001$ ".

## **Results**

#### *Changes in the gut microbiome in patient with FMT treatment*

A colonoscopy examination was used to detect the remission of colonic ulcers in a patient with UC after the FMT treatment (Figure 1). We also analyzed the microbiome composition of stool samples from this patient before and after the FMT treatment, and the results revealed that the population of *R. intestinalis* was increased after UC remission (Figure 1). The proportion of *R. intestinalis* was only 0.05% of the total microbiota before the FMT treatment and increased to 27.25% after UC remission (Figure 1). Based on this finding, we hypothesized that *R. intestinalis* might play an essential role in the recovery of patients with UC.

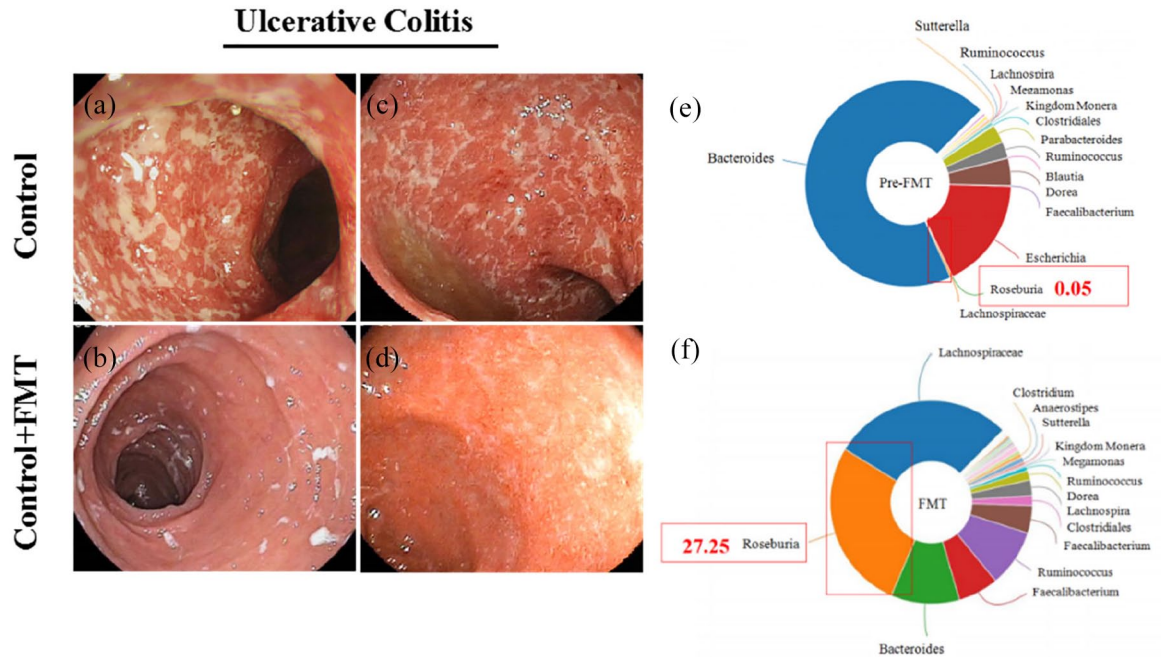


**Figure 1.** Comparison of colonoscopy pictures and intestinal bacterial composition of a patient receiving FMT. (a)–(d) Contrast colonoscopy photos of the same patient with UC after FMT treatment. (a) and (c) Colonoscopy pictures before FMT treatment, with diffuse and multiple ulcers on the colonic mucosa, as well as blurred blood vessels, a fragile texture, bleeding, and purulent secretions. The images shown in (b) and (d) were captured after FMT treatment, showing ulcer remission with pseudopolyps and a smoother mucosal layer. (e) Diagram of the composition of the fecal microbiota when the patient had not received FMT; (f) diagram of the composition of the fecal microbiota after the patient received FMT.

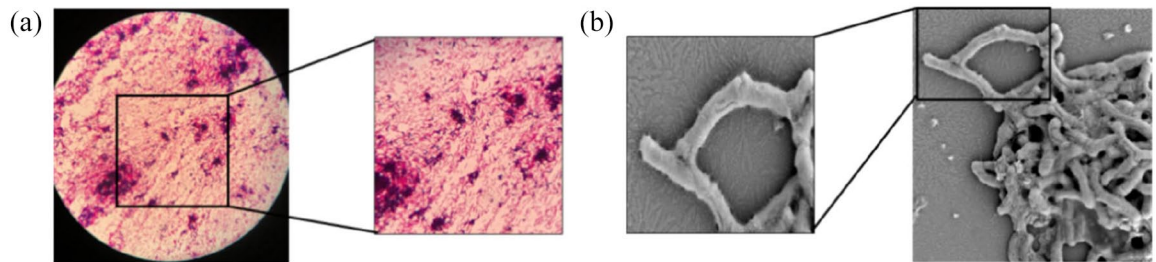


**Figure 2.** (a) Gram staining results showing that *R. intestinalis* is gram-variable. Red is generally considered to be gram-negative, and blue-violet is gram-positive. (b) Scanning electron microscopy images of *R. intestinalis*.

#### Identification and characterization of *R. intestinalis*

*R. intestinalis* is a saccharolytic, butyrate-producing bacterium that was first isolated from human feces.<sup>25</sup> In this study, Gram staining and SEM were first performed to assess the morphology of *R. intestinalis* (Figure 2). The SEM image showed a slightly crooked bacillus shape wrapped by

flagella for the strain used in this study (Figure 2), consistent with the distinctive characteristics of *R. intestinalis*.<sup>26</sup> We used the first three results from the NCBI database to compare the genome of the R.I strain and further assess and identify the strain used in this study. According to the results (Table 1), the strain used in our research shares the closest genetic relationship with *R. intestinalis*.

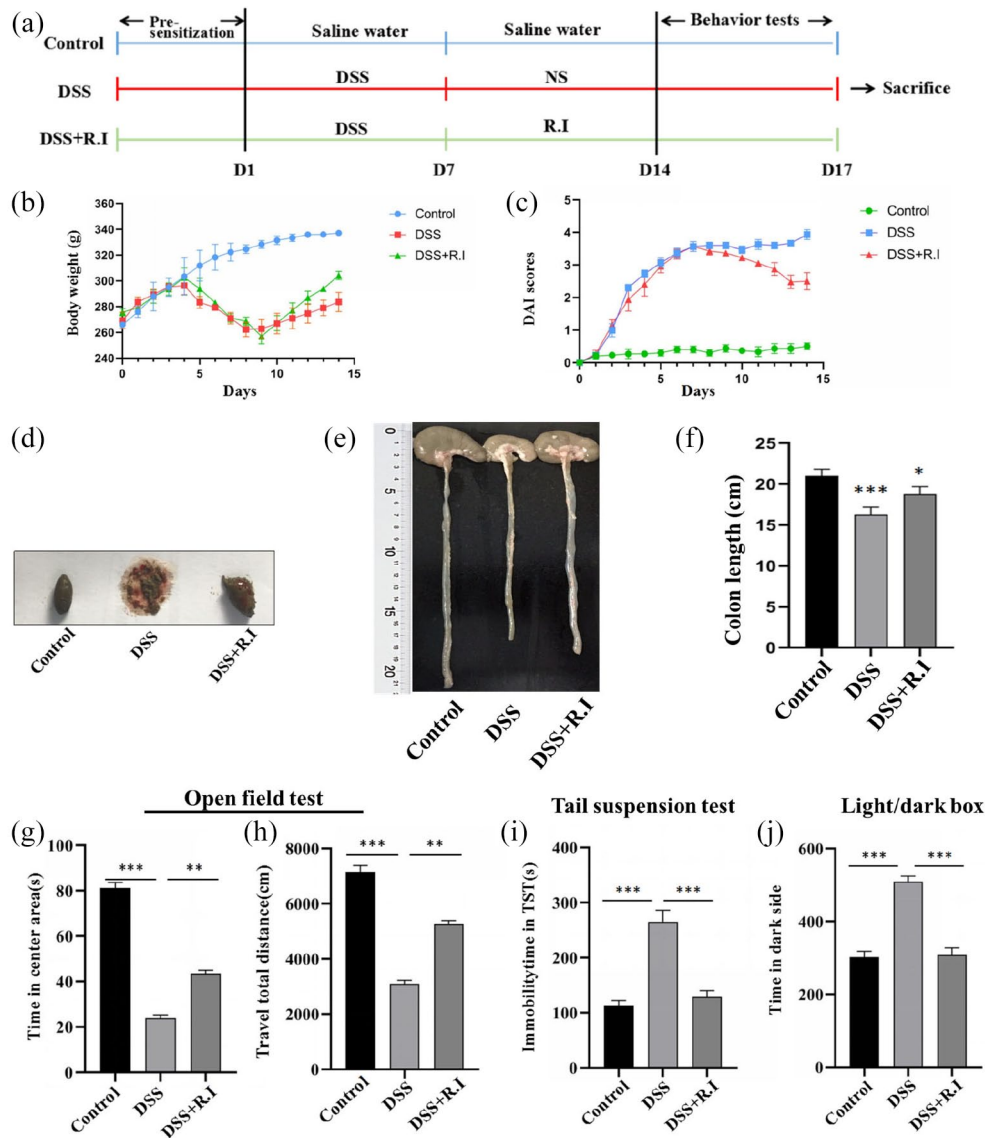


**Figure 3.** Health conditions of rats and colon histology. (a) Experimental design. (b) Body weight change in each group. (c) Disease activity index (DAI) scores of each group. (d) Fecal traits of each group. Stool samples were collected from each group on the 17th day. (e) The length of colon from rats in each group. (f) Comparison of colon length in each group of rats. (g) Time spent by rats in the center area during the open field test (OFT). (h) Effects of *R. intestinalis* on the total distance traveled by the DSS-treated rats in open field test (OFT). (i) Examination of immobility in the tail suspension test (TST). (j) Time spent by rats in the dark environment of the light/dark box (LDB). Data are presented as the means  $\pm$  SEM ( $n=6$  per group). The results were analyzed using one-way ANOVA. \* $p < 0.05$ , \*\* $p < 0.01$ , \*\*\* $p < 0.001$  compared with the DSS group.

### *R. intestinalis* improved health in colitis rats

During the period of DSS challenge, the body weight of rats with colitis in both the DSS and DSS + R.I groups was significantly decreased compared with the control group (Figure 3). When DSS stimulation was stopped, rats showed a recovery in body weight and the change in the DSS + R.I group was more rapid than in the DSS

group. The stool samples from each group also presented different characteristics. Feces from the DSS group appeared watery and bloody, but the stool samples from the *R. intestinalis*-treated rats showed healthier traits. The DAI scores of each group were recorded as well, which increased dramatically with DSS administration and then decreased after DSS was stopped accompanied

**Table 1.** Identification of *Roseburia intestinalis*.

Description	Max score	Total score	Query cover	Evalue	Per.Ident	Accession
<i>Roseburia intestinalis</i> gene for the 16S ribosomal RNA, partial sequence, strain: JCM 17583	2575	2575	100%	0	99.93%	AB661435.1
<i>Roseburia intestinalis</i> XB6B4 draft genome	2575	2575	100%	0	99.93%	FP929050.1
<i>Roseburia intestinalis</i> partial 16S rRNA gene, strain XB6B4	2575	2575	100%	0	99.93%	AM055815.1

The NCBI database was searched and the first three results were compared. According to the strain identification results, the strain used in this study shares the closest genetic relationship with *Roseburia intestinalis*.

by the *R. intestinalis* treatment (Figure 3). This result is consistent with the trend of the body weight, showing that *R. intestinalis* therapy induced colitis remission. When the week of *R. intestinalis* treatment ended, the rats were euthanized and dissected. The colon length of the rats in the DSS + R.I group was significantly longer than in the DSS group (Figure 3).

#### *R. intestinalis* has ameliorated depressive-like behaviors in colitis rats

Rats were subjected to behavioral tests at the end of treatment to evaluate whether the remission of colitis was accompanied by neuroprotective effects. We evaluated the locomotor activity of the rats using the OFT, TST and LDB assays, and significant differences were observed in all groups (Figure 3).

Specifically, the OFT, TST and LDB assays showed that the administration of *R. intestinalis* alleviated depressive and anxiety-like behaviors, such as poor performance in the OFT, longer immobility time in the TST, and remaining in the dark in the LDB, in rats with colitis.

#### The recovery of intestinal function induced by *R. intestinalis*

We next carried out 16S ribosomal RNA sequencing to assess the diversity and composition of the gut microbiota in rats from different groups. A heatmap of the operational taxonomic unit profiles showed variation before (DSS S) and after (DSS E) DSS challenge, while the abundance of the fecal microbiota from the rats in the DSS + R.I group showed insignificant changes before and after *R. intestinalis* treatment (Figure 4). Collinearity

diagrams and violin plots also revealed significant changes in the rats with DSS-induced colitis, but the *R. intestinalis* treatment abolished these changes (Figure 4). These results indicate that although gut dysbiosis occurs in rats with colitis, treatment with *R. intestinalis* efficiently restored a healthy microecology in the digestive system, contributing to functional recovery.

We performed histological assays to examine rats subjected to different treatments to further investigate the effect of *R. intestinalis* on restoring colon function. First, morphological changes in the colon and collagen fibers, which are representative indicators of gastrointestinal (GI) barrier function, were investigated. The rats in the DSS group exhibited sparse and short crypts and thin intestinal walls with increased numbers of collagen fibers (Figure 5). These abnormal structures indicate malfunctioning of the GI barrier and digestive system dysfunction. A qRT-PCR analysis of colon tissue revealed that the proinflammatory factors IL-6 and IL-17 were upregulated in rats with colitis but then decreased significantly after the *R. intestinalis* treatment (Figure 5). Moreover, 5-hydroxytryptamine (5-HT) expression in the DSS + R.I group was significantly decreased compared with the DSS-treated rats (Figure 5).

We examined the mucosal integrity and tight junctions of colon tissues from the rats in different groups by performing IHC assays and western blotting to further investigate the restoration of GI function mediated by the *R. intestinalis* treatment. The colons of rats treated with DSS exhibited significantly decreased expression of Zo-1, while the *R. intestinalis* treatment increased its expression levels (Figure 6).<sup>27</sup> GFAP was also

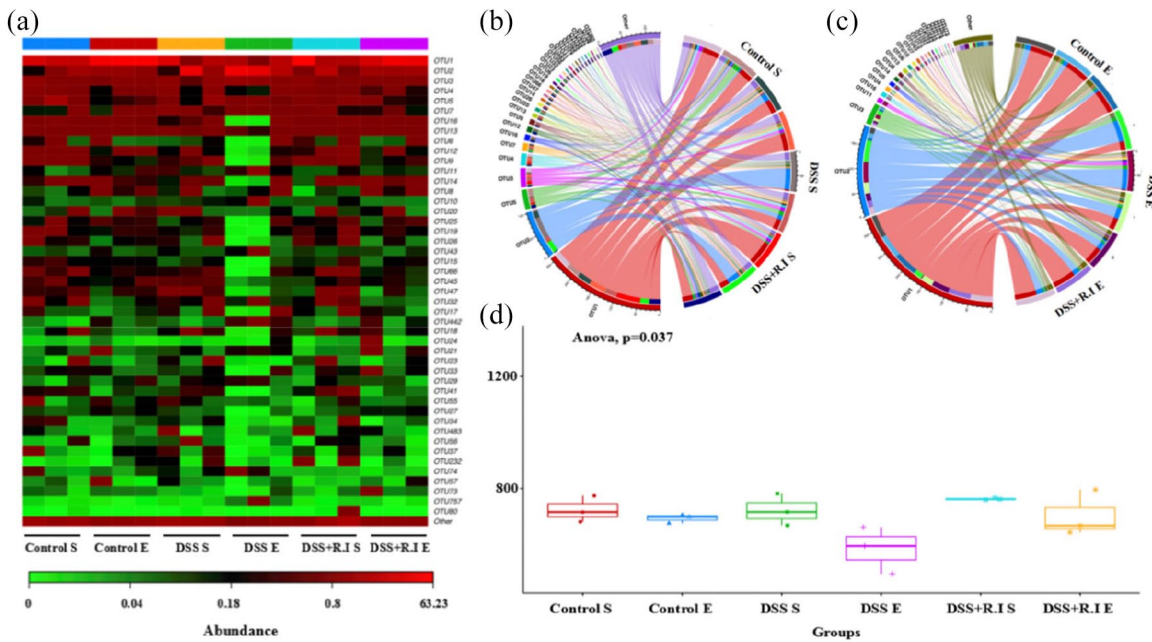


**Figure 4.** Effects of *R. intestinalis* on the intestinal microbiota of the DSS group. (a) Functional abundance heat map of the different groups. Each column in the figure represents a sample, and the color block represents the functional abundance value. Redder colors represent higher abundances, and greener colors represent lower abundances. (b) and (c) Collinearity diagrams of different groups. The semicircle on the right represents the species abundance in the sample, and the semicircle on the left represents the distribution of species in different samples. (d) The  $\alpha$ -diversity estimated using the Chao1 index in different groups; each box in the figure represents a group.

evaluated to confirm the recovery of the GI barrier mediated by *R. intestinalis* (Figure 6).<sup>28</sup>

#### *Anti-inflammatory effect of R. intestinalis on the central nervous system of rats with colitis*

As behavioral tests showed that *R. intestinalis* alleviated depressive-like symptoms in rats with colitis, we next studied the inflammatory condition in both serum and brain samples from all groups.

The ELISA of rat serum samples showed that both IL-6 and IL-17 were upregulated in the rats with colitis, but decreased in rats that underwent the *R. intestinalis* treatment (Figure 7), and a similar change was observed in rat brain tissues using qRT-PCR (Figure 7). Moreover, we used 5-hydroxytryptamine (5-HT) as an indicator of inflammatory cell activation, and the elevated levels of 5-HT detected in both serum and the brain were reversed by the *R. intestinalis* treatment (Figure 7). This synchronism of inflammatory regulators in both the serum and brain suggests that *R. intestinalis* potentially affects the gut–brain axis of rats with colitis.

The dorsal motor nucleus of the vagus nerve and the hypothalamus regulate the intestinal nervous and immune systems through nerves or neuroendocrine pathways, and their functions may also be affected by neuroinflammation due to the activation of microglia. Therefore, we examined the activation of microglia in the hypothalamus by performing Iba-1 IHC and western blotting. After the DSS challenge, microglial cells were activated and presented remarkably enlarged cellular bodies and hyper-ramified and thick processes; however, these alterations were alleviated in the DSS + R.I group (Figure 7). The quantification of Iba-1 was also confirmed through western blotting (Figure 7).

#### Discussion

Although the etiology and pathogenesis of UC have not been confirmed, the connection between gut microbiota dysbiosis and intestinal malfunction has been verified in many preclinical and clinical studies.<sup>13,29–31</sup> In this study, we found that the abundance of *R. intestinalis* differed in patients before and after UC remission, and, for the first

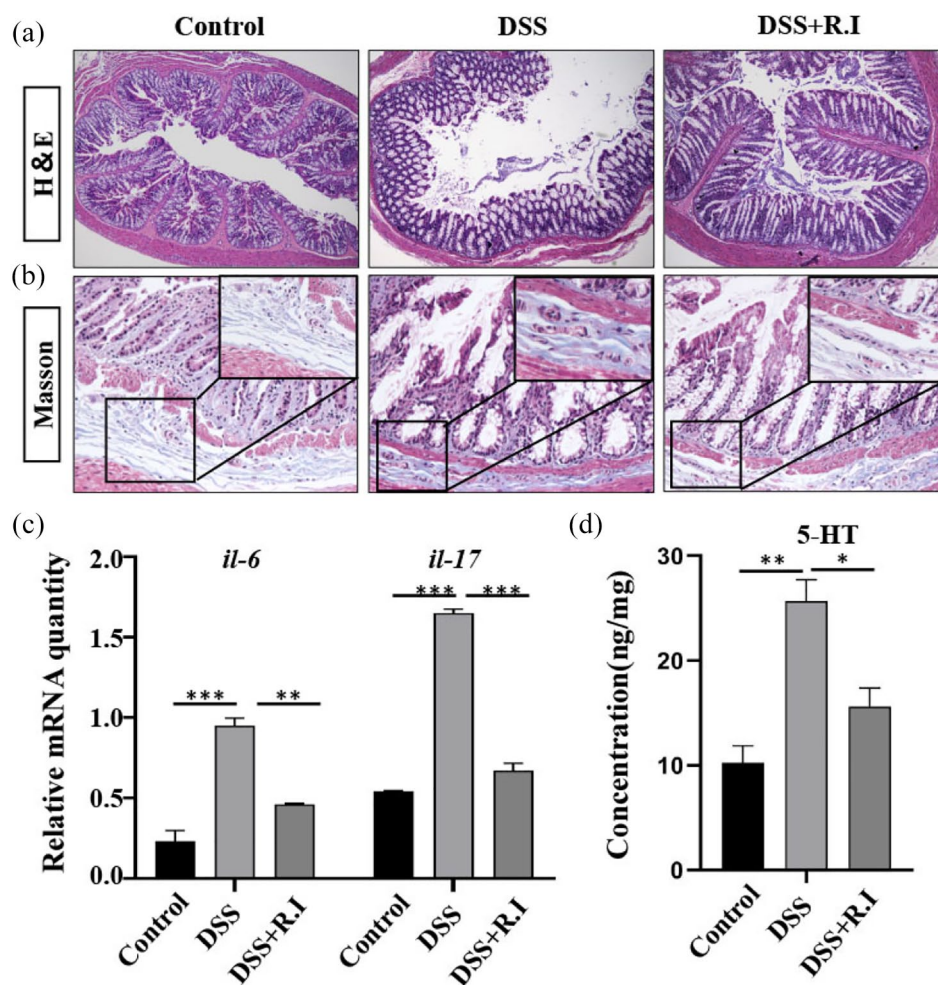


**Figure 5.** Representative images of changes in the intestinal morphology of each group. (a) Representative images of H&E-stained colon sections from rats with different treatments after 7 days. (b) Representative images of Masson's trichrome-stained colon sections from rats with different treatments after 7 days. Treatment with *R. intestinalis* alleviated mucosal lesions in the colon. (c) Relative measurement of colonic mRNA expression of IL-6 and IL-17 in rats. (d) The expression level of 5-HT in the colon was measured using an ELISA.

Data are presented as the means  $\pm$  SEM ( $n=3$  per group). The results were analyzed using one-way ANOVA. \* $p < 0.05$ , \*\* $p < 0.01$ , \*\*\* $p < 0.001$  compared with the DSS group.

time, we confirmed that probiotic therapy using *R. intestinalis* ameliorated colitis and neurological disorders by modulating the gut–brain axis.

FMT is regarded as an effective method for treating intractable inflammatory bowel diseases. Our group has been using this approach for a long time to treat patients with UC in clinical practice and has achieved desirable results. Moreover, colitis remission correlates with the relief of mental health disorders through the microbiota–gut–brain axis.<sup>23,32,33</sup> Based on our findings in clinical patients with UC, we hypothesized that exogenous

supplementation with *R. intestinalis* would improve intestinal function and the gut barrier, and neurological inflammation related to colitis would also be relieved. We performed a series of analyses of GI function, the gut microbiota and inflammation of the central nervous system in a colitis model to study the effect of *R. intestinalis* on the inflammatory cascade through the microbiota–gut–brain axis.

In this study, we constructed a colitis model in rats by administering DSS as a representative platform to study the effect of *R. intestinalis* on

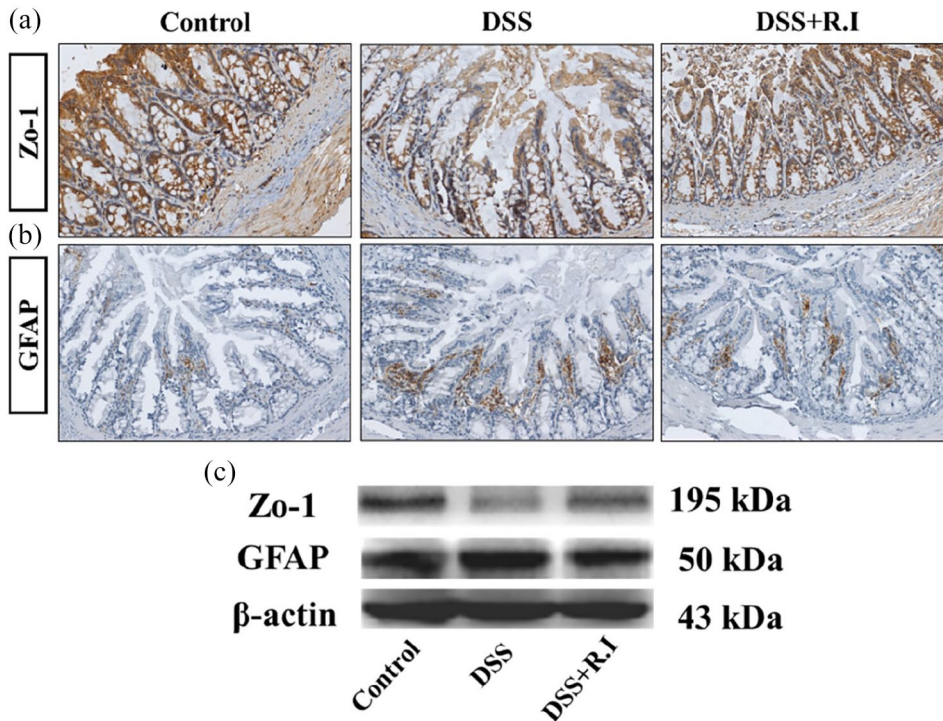


**Figure 6.** The expression of molecules related to the gut barrier. The astrocyte phenotype was assessed by performing GFAP IHC in the colon. Representative image of IHC staining for (a) Zo-1 and (b) GFAP in colonic mucosal epithelial cells of the control group, DSS group and DSS + R.I group. (c) Levels of the Zo-1 and GFAP proteins were analyzed using western blotting.

colitis. Murine models of various diseases and physiological dysfunctions are used in preclinical studies to study etiologies and pharmacological treatments, and the choice of an appropriate model with a strong connection and similarity would provide reliable evidence.<sup>34,35</sup> In a recent study that compared the gut metagenome between rats and mice with humans, the data showed a higher pairwise overlap in humans and rats than in mice and rats, where 97% of functional pathways in the human catalog were expressed in the rat catalog.<sup>36,37</sup>

Based on our results, *R. intestinalis* exerted a therapeutic effect on DSS-challenged rats. Sparse and short crypts with a thin intestinal mucosal layer in the rat colon, as well as the symptoms caused by colitis, were significantly relieved by the *R. intestinalis* treatment, and the greater number of collagen fibers in colon tissue also suggested a protective effect on GI function and gut barrier recovery. To our knowledge, the gut barrier plays a vital role in the interaction between the enteric environment and extraintestinal

functions.<sup>38</sup> In UC, a disrupted gut barrier is not sufficient to block enteric toxins or proinflammatory regulators from entering the extraintestinal system, and disorders of distant tissues are thus induced. Among these disorders, neurological inflammation and mental disorders are typical extraintestinal responses caused by UC through the gut–brain axis.<sup>33</sup>

We also investigated behavioral changes in rats to study whether *R. intestinalis* could be applied as a therapeutic agent to relieve UC and neuroinflammation by modulating the gut–brain axis. Our data showed that DSS induced depressive-like behavior in rats with colitis, while the *R. intestinalis* treatment relieved these symptoms. Moreover, treatment with *R. intestinalis* altered the gut microbiota composition and diversity. This change in the fecal microbiota indicates the restoration of the gut microecology, which is essential for maintaining a balanced intestinal microenvironment.<sup>39</sup> Further analyses of intestinal function and the colonic barrier using western blotting and IHC indicated the recovery of the

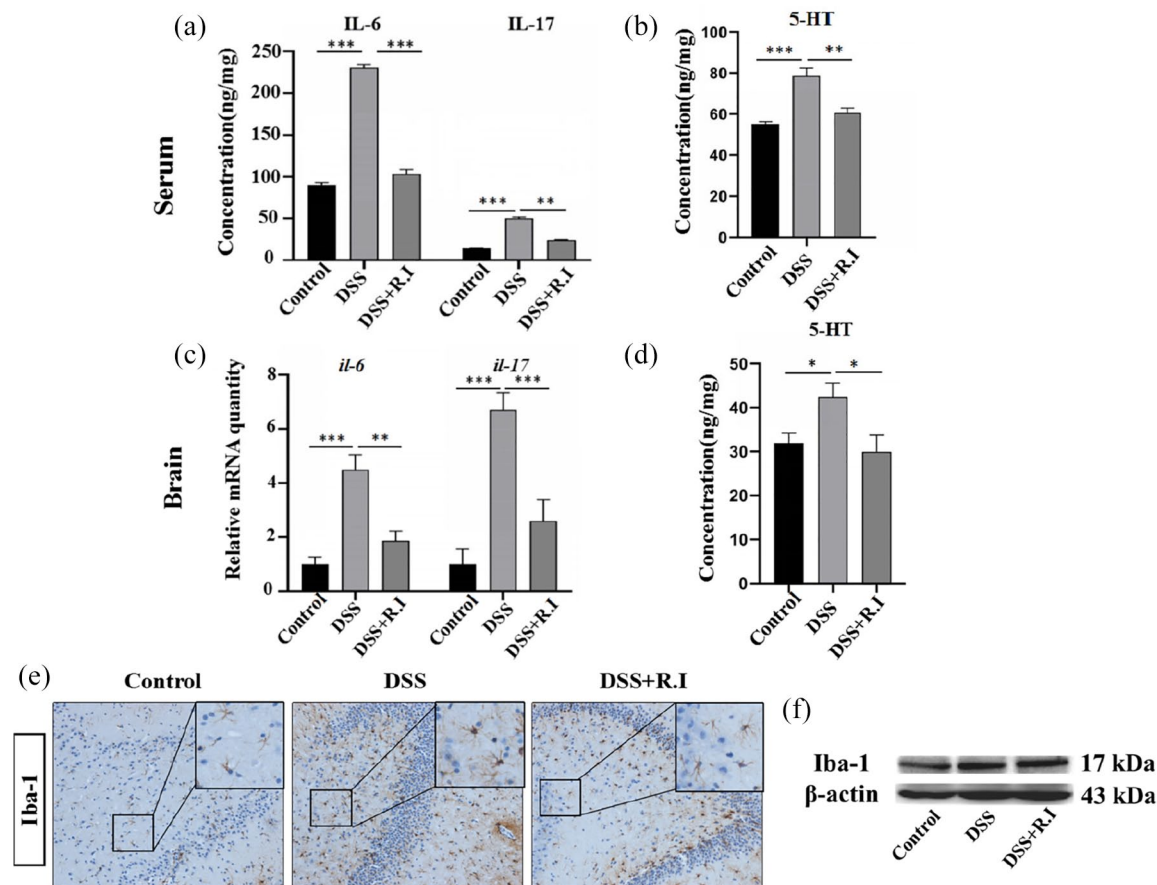


**Figure 7.** The effects of *R. intestinalis* on rats with colitis. The levels of (a) IL-6, IL-17, and (b) 5-HT in serum were detected using ELISAs. (c) Expression of the IL-6 and IL-17 mRNAs in rat brains evaluated using RT-qPCR. (d) 5-HT concentrations in the brain were measured using an ELISA. (e) The activation of microglial cells in the hypothalamus and dorsal motor nucleus of the vagus nerve. (f) Levels of the Iba-1 protein were analyzed using western blotting.

Data are presented as the means  $\pm$  SEM ( $n=3$  per group). The results were analyzed using one-way ANOVA. \* $p < 0.05$ , \*\* $p < 0.01$ , \*\*\* $p < 0.001$  compared with the DSS group.

epithelial structure, suggesting that *R. intestinalis* exerts a protective effect on the gut barrier in rats with colitis by restoring the gut microbiota. The evaluation of GFAP as an indicator of an intact functional intestinal barrier is also consistent with the abovementioned results.<sup>40,41</sup>

Furthermore, the changes in the levels of IL-6 and IL-17 in both serum and brain also suggests an effect of *R. intestinalis* on the gut–brain axis. A similar change was observed in the expression of 5-HT, a neurotransmitter that extensively affects cerebral activity and modulates emotion and memory, acting as a mediator in neuronal networks through the gut–brain axis.<sup>42</sup> IHC and western blotting results both illustrated that

microglial cells were activated after DSS challenge, while this activation was reversed by *R. intestinalis* administration, indicating that *R. intestinalis* exerted a protective effect on the central nervous system through the gut–brain axis.

In conclusion, this study is the first to report the therapeutic and protective effects of *R. intestinalis* on UC and neurological disorders. Our data together suggest that *R. intestinalis* might serve as a beneficial treatment for the establishment and maintenance of a healthy gut microbiota, contributing to the restoration of the intestinal barrier, and it might exert a protective effect on colitis-related brain inflammation through the microbiota–gut–brain axis.

## Acknowledgements

Not applicable.

## Conflict of interest statement

The authors declare that there is no conflict of interest.

## Funding

The authors disclosed receipt of the following financial support for the research, authorship, and/or publication of this article: This work was supported by the Science and Technology Innovation Project, the Military Scientific Committee of the People's Liberation Army of China (17-163-12-ZT-002-060-01); Medical Science and Technology Pilot Project for Youth Investigators, the Military Scientific Committee of the People's Liberation Army of China (16QNP098); and the Frontier Innovation Capability Cultivation Program of Army Medical Center of PLA (2019CXJSB008).

## Research ethics and patient consent

The study protocol was approved by the Department of Gastroenterology, Daping Hospital (Medical Research Ethics 2014. Number 17), and all subjects provided written informed consent prior to participating in the study.

## ORCID iD

Yanling Wei  <https://orcid.org/0000-0002-3307-3092>

## References

1. Ordas I, Eckmann L, Talamini M, *et al.* Ulcerative colitis. *Lancet* 2012; 380: 1606–1619.
2. Yu YR and Rodriguez JR. Clinical presentation of Crohn's, ulcerative colitis, and indeterminate colitis: symptoms, extraintestinal manifestations, and disease phenotypes. *Semin Pediatr Surg* 2017; 26: 349–355.
3. Borren NZ, Van Der Woude CJ and Ananthakrishnan AN. Fatigue in IBD: epidemiology, pathophysiology and management. *Nat Rev Gastroenterol Hepatol* 2019; 16: 247–259.
4. Graff LA, Walker JR and Bernstein CN. Depression and anxiety in inflammatory bowel disease: a review of comorbidity and management. *Inflamm Bowel Dis* 2009; 15: 1105–1118.
5. Marafini I, Longo L, Lavasani DM, *et al.* High frequency of undiagnosed psychiatric disorders in inflammatory bowel diseases. *J Clin Med* 2020; 9: 1387.
6. Bernstein CN, Hitchon CA, Walld R, *et al.* Increased burden of psychiatric disorders in inflammatory bowel disease. *Inflamm Bowel Dis* 2019; 25: 360–368.
7. Ballou S and Keefer L. Psychological interventions for irritable bowel syndrome and inflammatory bowel diseases. *Clin Transl Gastroenterol* 2017; 8: e214.
8. Tarricone I, Regazzi MG, Bonucci G, *et al.* Prevalence and effectiveness of psychiatric treatments for patients with IBD: a systematic literature review. *J Psychosom Res* 2017; 101: 68–95.
9. Ananthakrishnan AN, Bernstein CN, Iliopoulos D, *et al.* Environmental triggers in IBD: a review of progress and evidence. *Nat Rev Gastroenterol Hepatol* 2018; 15: 39–49.
10. Sun L, Nava GM and Stappenbeck TS. Host genetic susceptibility, dysbiosis, and viral triggers in inflammatory bowel disease. *Curr Opin Gastroenterol* 2011; 27: 321–327.
11. Zhang YZ and Li YY. Inflammatory bowel disease: pathogenesis. *World J Gastroenterol* 2014; 20: 91–99.
12. Sokol H, Leducq V, Aschard H, *et al.* Fungal microbiota dysbiosis in IBD. *Gut* 2017; 66: 1039–1048.
13. Ni J, Wu GD, Albenberg L, *et al.* Gut microbiota and IBD: causation or correlation? *Nat Rev Gastroenterol Hepatol* 2017; 14: 573–584.
14. Kostic AD, Xavier RJ and Gevers D. The microbiome in inflammatory bowel disease: current status and the future ahead. *Gastroenterology* 2014; 146: 1489–1499.
15. Bernstein CN. Treatment of IBD: where we are and where we are going. *Am J Gastroenterol* 2015; 110: 114–126.
16. Sparrow MP, Irving PM and Hanauer SB. Optimizing conventional therapies for inflammatory bowel disease. *Curr Gastroenterol Rep* 2009; 11: 496–503.
17. Abraham BP and Quigley EMM. Probiotics in inflammatory bowel disease. *Gastroenterol Clin North Am* 2017; 46: 769–782.
18. Duncan SH, Hold GL, Barcenilla A, *et al.* *Roseburia intestinalis* sp. nov., a novel saccharolytic, butyrate-producing bacterium from

- human faeces. *Int J Syst Evol Microbiol* 2002; 52: 1615–1620.
19. Louis P and Flint HJ. Diversity, metabolism and microbial ecology of butyrate-producing bacteria from the human large intestine. *FEMS Microbiol Lett* 2009; 294: 1–8.
  20. Zhu C, Song K, Shen Z, *et al.* *Roseburia intestinalis* inhibits interleukin17 excretion and promotes regulatory T cells differentiation in colitis. *Mol Med Rep* 2018; 17: 7567–7574.
  21. Shen Z, Zhu C, Quan Y, *et al.* Insights into *Roseburia intestinalis* which alleviates experimental colitis pathology by inducing anti-inflammatory responses. *J Gastroenterol Hepatol* 2018; 33: 1751–1760.
  22. Cooper HS, Murthy SN, Shah RS, *et al.* Clinicopathologic study of dextran sulfate sodium experimental murine colitis. *Lab Invest* 1993; 69: 238–249.
  23. Liu Y, Xu F, Liu S, *et al.* Significance of gastrointestinal tract in the therapeutic mechanisms of exercise in depression: synchronism between brain and intestine through GBA. *Prog Neuropsychopharmacol Biol Psychiatry* 2020; 103: 109971.
  24. Guida F, Boccella S, Iannotta M, *et al.* Palmitoylethanolamide reduces neuropsychiatric behaviors by restoring cortical electrophysiological activity in a mouse model of mild traumatic brain injury. *Front Pharmacol* 2017; 8: 95.
  25. Luo W, Shen Z, Deng M, *et al.* *Roseburia intestinalis* supernatant ameliorates colitis induced in mice by regulating the immune response. *Mol Med Rep* 2019; 20: 1007–1016.
  26. Xiao M, Shen Z, Luo W, *et al.* A new colitis therapy strategy via the target colonization of magnetic nanoparticle-internalized *Roseburia intestinalis*. *Biomater Sci* 2019; 7: 4174–4185.
  27. Han X, Lee A, Huang S, *et al.* *Lactobacillus rhamnosus* GG prevents epithelial barrier dysfunction induced by interferon-gamma and fecal supernatants from irritable bowel syndrome patients in human intestinal enteroids and colonoids. *Gut Microbes* 2019; 10: 59–76.
  28. Ma EL, Smith AD, Desai N, *et al.* Bidirectional brain-gut interactions and chronic pathological changes after traumatic brain injury in mice. *Brain Behav Immun* 2017; 66: 56–69.
  29. Nishida A, Inoue R, Inatomi O, *et al.* Gut microbiota in the pathogenesis of inflammatory bowel disease. *Clin J Gastroenterol* 2018; 11: 1–10.
  30. Lin L and Zhang J. Role of intestinal microbiota and metabolites on gut homeostasis and human diseases. *BMC Immunol* 2017; 18: 2.
  31. Imhann F, Vich Vila A, Bonder MJ, *et al.* Interplay of host genetics and gut microbiota underlying the onset and clinical presentation of inflammatory bowel disease. *Gut* 2018; 67: 108–119.
  32. Zhao X, Cao F, Liu Q, *et al.* Behavioral, inflammatory and neurochemical disturbances in LPS and UCMS-induced mouse models of depression. *Behav Brain Res* 2019; 364: 494–502.
  33. Dinan TG and Cryan JF. The microbiome-gut-brain axis in health and disease. *Gastroenterol Clin North Am* 2017; 46: 77–89.
  34. Eichele DD and Kharbanda KK. Dextran sodium sulfate colitis murine model: an indispensable tool for advancing our understanding of inflammatory bowel diseases pathogenesis. *World J Gastroenterol* 2017; 23: 6016–6029.
  35. Chassaing B, Aitken JD, Malleshappa M, *et al.* Dextran Sulfate Sodium (DSS)-induced colitis in mice. *Curr Protoc Immunol* 2014; 104: 15.25.1–15.25.14.
  36. Pan H, Guo R, Zhu J, *et al.* A gene catalogue of the Sprague-Dawley rat gut metagenome. *Gigascience* 2018; 7: giy055.
  37. Lleal M, Sarrabayrouse G, Willamil J, *et al.* A single faecal microbiota transplantation modulates the microbiome and improves clinical manifestations in a rat model of colitis. *EBioMedicine* 2019; 48: 630–641.
  38. Hsu YC, Wu TC, Lo YC, *et al.* Gastrointestinal complications and extraintestinal manifestations of inflammatory bowel disease in Taiwan: a population-based study. *J Chin Med Assoc* 2017; 80: 56–62.
  39. Marchesi JR, Adams DH, Fava F, *et al.* The gut microbiota and host health: a new clinical frontier. *Gut* 2016; 65: 330–339.
  40. Hu S, Zhao ZK, Liu R, *et al.* Electroacupuncture activates enteric glial cells and protects the gut barrier in hemorrhaged rats. *World J Gastroenterol* 2015; 21: 1468–1478.
  41. Yu YB and Li YQ. Enteric glial cells and their role in the intestinal epithelial barrier. *World J Gastroenterol* 2014; 20: 11273–11280.
  42. Xi TF, Li DN, Li YY, *et al.* Central 5-hydroxytryptamine (5-HT) mediates colonic motility by hypothalamus oxytocin-colonic oxytocin receptor pathway. *Biochem Biophys Res Commun* 2019; 508: 959–964.